Computation of Decaying Wall-Stabilized Arcs *

W. HERMANN

Brown Boveri Research Center, CH-5401 Baden, Switzerland

(Z. Naturforsch. **28 a**, 443—453 [1973]; received 27 October 1972)

The interaction between an electric arc and a gas flow is governed by the flow of mass relative to surfaces of constant temperature. This fact is used to introduce a new method for the computation of decaying wall-stabilized arcs in which the temperature is used as a free variable instead of the radial coordinate. The method is also applicable to more general cases and gives direct insight into the physical processes involved. An implicit two level scheme is described which guarantees numerical stability for any chosen time step. The method is applied to a decaying wall stabilized arc. The results agree quite well with published experimental curves.

I. Introduction

There is a general interest in both the stationary and the dynamic behaviour of electric arcs because of different important technical applications and due to the fact that this type of plasma can be produced and studied in relatively simple geometries. A large number of papers has been published on the stationary wall-stabilized arc dealing mostly with the evaluation of material functions from arc measurements [1–5].

Fewer papers deal with the dynamic behaviour of wall-stabilized arcs [6–10], although the time variation of such a simple type of arc readily reveals the main features of nonstationary arc behaviour. In this paper a new method for the computation of decaying wall-stabilized arcs is presented. The method is also applicable to more general cases, but in this particular example it clearly shows the principle underlying the interaction between electric arcs and gas flow, i. e. the importance of the flow of mass relative to the isothermal surfaces [11, 12]. The method described is an improvement of the computation of decaying arcs due to its simple form, its stability in numerical calculations and its ability to illustrate the underlying physical processes. The computations are performed for a 5 mm ϕ, wall-stabilized arc, which carries a current of 100 A in 1 atm nitrogen. All important physical mechanisms are included such as heat conduction and convective and radiative transport. For this special example experimental results have been published [10], which can be used for comparison.

Reprint requests to Dr. W. HERMANN, Brown Boveri Research Center, *CH-5401 Baden* (Schweiz).

* *Herrn Prof.* H. MAECKER *zum 60. Geburtstag gewidmet.*

II. Basic Equations and Physical Picture

The arc considered here has cylindrical symmetry. There is no axial mass velocity, so the axial momentum balance can be omitted. The radial balance of momentum is neglected since radial pressure gradients are equalized on a time scale short compared to the decay time. Therefore the total arc behaviour is described by the conservation of mass and energy:

$$\frac{\partial \varrho}{\partial t} + \frac{1}{r}\frac{\partial}{\partial r}(r\, v_r\, \varrho) = 0\,, \tag{1}$$

$$\frac{\partial}{\partial t}(\varrho\, \varepsilon) + \frac{1}{r}\frac{\partial}{\partial r}(r\, v_r\, \varrho\, h) \tag{2}$$
$$= \varrho\left(\frac{\partial h}{\partial t} + v_r \frac{\partial h}{\partial r}\right) - \frac{\partial p}{\partial t} = \sigma E^2 - u + \frac{1}{r}\frac{\partial}{\partial r}\left(r \varkappa \frac{\partial T}{\partial r}\right).$$

The symbols used here are: T temperature, E electrical field strength, v_r radial mass velocity, ϱ mass density, $\varkappa$ thermal conductivity, σ electrical conductivity, h enthalpy. The internal energy ε is given by $\varepsilon = h - p/\varrho$. The term u is the balance between the radiative power "e" emitted and "a" absorbed per unit volume

$$u = e - a\,. \tag{3}$$

We consider the decay of an originally stationary arc after current interruption, i.e. after the term σE^2 in Eq. (2) has dropped to zero. The process is described by the system of non-linear parabolic Eqs. (1) and (2). It can be formulated as an initial value problem and is solved by starting from a stationary distribution at time zero.

The stationary arc is described by the right hand side of Equation (2). The energy supplied by ohmic heating is carried away by conduction and radiation. The temperature profile is curved in such a

way that the energy flow by conduction, together with the radiative energy flow across a certain radius r equals the energy input by ohmic heating within the area enclosed by r:

$$2\pi\left(-r\varkappa\frac{\partial T}{\partial r}\right)+2\pi\int_0^r u\,r\,\mathrm{d}r=2\pi\int_0^r\sigma E^2 r\,\mathrm{d}r\,. \tag{2 a}$$

In the time immediately after current interruption the heating term has disappeared, but the temperature profile still maintains its original form. Therefore the radiative and conductive transport terms keep their old distribution and the same amount of energy is carried across each radius by conduction and radiation as before arc interruption. This loss of energy causes a decrease of the energy content within the observed radius and therefore a decrease in local temperature. The temperature profile is therefore changed and with it the transport terms.

In the inner part of the arc the mass density rises strongly with falling temperature and a radial mass flow from the wall region towards the core of the arc is established. It is assumed that the arc vessel is closed and so the total pressure drops slowly. The induced radial velocity also influences the energy balance as can be seen from Equation (2). If there is a local change of enthalpy the convection term describes an additional cooling as the inflowing colder gas is heated up.

The two terms $\partial h/\partial t$ and $v_\mathrm{r}\,\partial h/\partial r$ of Eq. (2) describe the change of enthalpy $\mathrm{D}h/\mathrm{D}t$ which is observed in a coordinate system moving with a mass element. These two terms can be substituted by one single term if the velocity of mass relative to the isothermal surfaces of a given temperature distribution, v_MI, is introduced:

For simplicity of discussion the pressure dependence of the enthalpy is dropped and the term $\mathrm{D}h/\mathrm{D}t$ can be represented by the change of enthalpy with respect to temperature times the change of temperature along the path of the element.

$$\frac{\partial h}{\partial t}+v_\mathrm{M}\frac{\partial h}{\partial r}=\frac{\mathrm{D}h}{\mathrm{D}t}=\frac{\mathrm{d}h}{\mathrm{d}T}\frac{\mathrm{D}T}{\mathrm{D}t}=c_p\frac{\mathrm{D}T}{\mathrm{D}t}\,. \tag{4 a}$$

Here the abbreviation v_M is used instead of v_r to stress the meaning of v_r as the velocity of mass, which, like all other velocities in the described example has only a radial component. c_p is the specific heat at constant pressure.

Given a radial temperature distribution the change of temperature along the path of a mass element, $\mathrm{D}T/\mathrm{D}t$, can be viewed as the product of the local change of temperature with radius, $\partial T/\partial r$, times the velocity of the mass element relative to the temperature distribution, i. e. relative to the isothermal surfaces, v_MI.

$$\frac{\mathrm{D}T}{\mathrm{D}t}=\frac{\partial T}{\partial r}v_\mathrm{MI}\,. \tag{5 a}$$

Then Eq. (4 a) reads:

$$\frac{\partial h}{\partial t}+v_\mathrm{M}\frac{\partial h}{\partial r}=c_p\frac{\partial T}{\partial r}v_\mathrm{MI}\,. \tag{4 b}$$

Only if mass moves relative to the temperature distribution does the enthalpy of a mass element change and does the term described by Eq. (4 b) become effective in the total energy balance. If the temperature distribution is carried with the gas flow (frozen temperature distribution) no gas is heated up and the term corresponding to Eq. (4 a) disappears from the energy balance. On the other hand this term also becomes effective if the temperature distribution moves relative to the stationary gas, since gas is again heated up. Whenever the stationary energy balance is no longer fulfilled a flow of the isothermal surfaces relative to mass is set up to balance the other terms in the energy equation. In the case of the decaying wall-stabilized arc, for instance, immediately after current interruption the ohmic heating term disappears in the core of the arc and a high relative velocity of mass against the isothermal surfaces will be established there. In the region close to the wall the energy balance is undisturbed; there the relative velocity is zero and the temperature distribution is carried with the mass flow.

If the absolute velocity of the isothermal surfaces

$$v_\mathrm{I}=\partial r_\mathrm{I}/\partial t$$

is introduced, the velocity of mass relative to the isothermal surfaces is given by the difference between both absolute velocities, v_M and v_I:

$$v_\mathrm{MI}=v_\mathrm{M}-v_\mathrm{I}\,. \tag{6}$$

The velocity of the isothermal surfaces represents the local variation of temperature with time:

$$\frac{\partial T}{\partial t}=-\frac{\partial T}{\partial r}\frac{\partial r_\mathrm{I}}{\partial t}=-\frac{\partial T}{\partial r}v_\mathrm{I}\,. \tag{5 b}$$

The introduction of the velocity of the isothermal surfaces greatly simplifies the computation of other

types of arcs, besides decaying arcs. This velocity appears directly when a transformation to a coordinate system is performed in which the temperature replaces the radius as an independent variable.

III. Isothermal Representation

The system of a decaying cylindrical arc is described by the two independent variables radius r and time t. As the temperature increases continuously from the wall towards the arc axis there is a one to one correspondence between the radius and the temperature, and the radius can be replaced by the temperature as a free variable. Instead of asking for the temperature at a certain r_i and t_j, $T(r_i, t_j)$ in this representation with T and t as free variables, one asks for the radius corresponding to a certain temperature T_i, at a certain time t_j, $r(T_i, t_j)$. This means that one follows the moving isothermal surfaces. In this system the described initial value problem is solved by computing at every time level the variation with time of the radii of the isothermal surfaces, $\partial r_i/\partial t$, which yields by some integration procedure the position of the isothermal surfaces at an advanced time level. Besides the simplification of the whole computation there are two main advantages to this transformation. Firstly the non-linearity of the equations due to the temperature dependence of the material functions disappears. Secondly, the choice of radial grid points which are equidistant in temperature ensures an optimal resolution of the radial profiles at any time. In the core of the arc only a few mesh points are used while in the outer region, where the temperature changes rapidly with radius, a large number of mesh points is used within a certain radial distance. This fact becomes even more important in the computation of axially blown arcs since in this case the temperature stays nearly constant over a large section of the arc core while it drops from this core value to the cold gas value within a very short radial distance [13]. There an adequate mesh point distribution is maintained even if, in the case of a decaying arc, this region of steep temperature gradients moves towards the arc axis. The general procedure and advantages of such a transformation are described in [12].

In the simple case considered here the basic equations can be transformed to the new coordinate system directly. The space derivative in the old coordinate system has to be replaced by the derivative with respect to temperature. However, in both cases the derivative must be performed perpendicular to the time coordinate, i. e. in pure radial direction and so one can still use the old abbreviation $(\partial/\partial r)_t$ in the new coordinate system.

The time derivative has to be carried out along an isothermal line, i. e. one has to add to the change with time at constant radius a term representing the change due to the radial displacement of an isothermal line:

$$\left(\frac{\partial}{\partial t}\right)_T = \left(\frac{\partial}{\partial t}\right)_r + \frac{\partial r_I}{\partial t}\left(\frac{\partial}{\partial r}\right)_t = \left(\frac{\partial}{\partial t}\right)_r + v_I\left(\frac{\partial}{\partial r}\right)_t. \quad (7)$$

Replacing the time derivative $(\partial/\partial t)_r$ in Eq. (2) by Eq. (7):

$$\frac{\partial h}{\partial r}\varrho(v_M - v_I) - \frac{dp}{dt} + \varrho\left(\frac{\partial h}{\partial t}\right)_T = \sigma E^2 - u + \frac{1}{r}\frac{\partial}{\partial r}\left(r\varkappa\frac{\partial T}{\partial r}\right). \quad (2\,b)$$

On the left hand side the relative velocity between mass and the isothermal surface, v_{MI}, appears. Multiplication of this velocity by the density ϱ times the circumference $2\pi r_i$ yields the mass flow per unit arc length across the isothermal surface at radius r_i:

$$q_{r_i} = 2\pi r_i \varrho(v_M - v_I) = 2\pi r_i \varrho v_{MI}. \quad (8)$$

If the relative mass flow, q, is isolated in Eq. (2 b) one obtains

$$q = \frac{2\pi r}{\partial h/\partial r}\left[\sigma E^2 - u + \frac{1}{r}\frac{\partial}{\partial r}\left(\varkappa r\frac{\partial T}{\partial r}\right)\right] + \frac{2\pi r}{\partial h/\partial r}\left(1 - \varrho\frac{\partial h}{\partial p}\right)\frac{dp}{dt}. \quad (8\,a)$$

The quantity q is determined by the balance of all energy terms except those due to convection and the local variation of temperature with time. It becomes effective only if this balance is disturbed. This is the case, for example, if one starts from the stationary arc, where the term in brackets is zero, and the ohmic heating term is dropped.

As a time variation of enthalpy along an isothermal surface can only be due to a change in pressure, no time derivative appears in Eq. (8 a) except

dp/dt. The term dp/dt is assumed constant over the whole arc cross section and is determined from the conservation of total mass. Assuming the value dp/dt to be known, the q_i at each isotherm can be computed directly for any given radial temperature distribution according to Equation (8 a).

To obtain the radial temperature distribution at an advanced time level one has to determine the time variation of the isothermal radii, $\partial r_i/\partial t$, i. e. the velocity of the isothermal surfaces, v_I, for the given distribution. This is possible using the conservation of mass once the values q_i are known.

To compute $\partial r_i/\partial t$ in an isothermal finite difference system it is advantageous to start from an integrated form of the mass balance. This is obtained in the new coordinate system if Eq. (1) is integrated over an arc cross-section limited, not by an independent value of radius r, but by a radius $r_i(T_i)$ corresponding to a temperature T_i:

$$2\pi \int_0^{r(T_i)} \frac{\mathrm{d}\varrho}{\partial t} r \,\mathrm{d}r + 2\pi \int_0^{r(T_i)} \frac{1}{r} \frac{\partial (r\,\varrho\, v_M)}{\partial r} r \,\mathrm{d}r = 0 . \quad (1\,a)$$

Taking into account the fact that the limit of integration, $r(T_i)$, is a dependent variable, whereas the radial coordinate, r, within the integral is not, this equation can be transformed to

$$\frac{\partial}{\partial t} 2\pi \int_0^{r_i} \varrho\, r \,\mathrm{d}r - 2\pi r_i \frac{\partial r_i}{\partial t} \varrho + 2\pi r_i \varrho\, v_M = 0 . \quad (1\,b)$$

With the definition for the mass flow relative to an isothermal surface, q_r , this reads:

$$\frac{\partial}{\partial t} 2\pi \int_0^{r_i} \varrho\, r \,\mathrm{d}r + q_{r_i} = 0 . \quad (1\,c)$$

If the values q_i are known this equation yields the required time variations, $\partial r_i/\partial t$, as wil be shown in detail in the next chapter.

IV. Method of Computation

The domain of solution is subdivided by a net which is made up of lines of equal temperature T_i and lines of equal time t_j:

$$T_i = T_w + (i-1)\,\Delta T ,$$
$$t_j = t_0 + j\,\Delta t . \quad (9)$$

Here $T_w = T_1$ is the wall temperature and t_0 is the time at which the decay of the arc starts.

Starting from the distribution at the time t_0 and advancing from time level t_j to time level t_{j+1} the value of the isothermal radius $r_{i,j+1}$ must be determined for every grid point. To do so the time variation of all isothermal radii, $\partial r_i/\partial t$, is computed at a given time level t_j and then the values of the isothermal radii at the advanced time level t_{j+1} are determined by an integration procedure. Along an isothermal surface the time-variation of the squared radius changes very little compared to that of the radius itself; therefore the variation of $r^2_{i,j}$ rather than of $r_{i,j}$ is computed.

The time variations $\partial r_i^2/\partial t$ are obtained for a given temperature distribution if Eq. (1 c) is written down for an area limited by two neighbouring isothermal surfaces:

$$q_i - q_{i-1} = \frac{\partial}{\partial t} \pi \int_{r_i^2}^{r^2_{i-1}} \varrho \,\mathrm{d}r^2 = \frac{\partial}{\partial t} (\bar{\varrho}_i A_i)$$
$$= \bar{\varrho}_i \frac{\partial A_i}{\partial t} + A_i \frac{\partial \bar{\varrho}_i}{\partial p} \frac{\mathrm{d}p}{\mathrm{d}t} . \quad (1\,d)$$

Here A_i is the area perpendicular to the arc axis between the two isothermal surfaces at $r^2(T_i)$ and $r^2(T_{i-1})$ and $\bar{\varrho}_i$ is the mean value of the density within this area. As the temperature stays constant in time between two isotherms, the density varies only with pressure. The values of q_i are known from Eq. (8) and the temporal variation of the areas between isothermal surfaces can be computed:

$$\frac{\partial A_i}{\partial t} = \pi \left(\frac{\partial r^2_{i-1}}{\partial t} - \frac{\partial r_i^2}{\partial t} \right)$$
$$= \frac{1}{\varrho_i} \left[q_i - q_{i-1} - A_i \frac{\partial \bar{\varrho}_i}{\partial p} \frac{\mathrm{d}p}{\mathrm{d}t} \right] . \quad (1\,e)$$

To determine the required quantities, $\partial r_i^2/\partial t$, from this equation one must know a boundary value of this quantity.

The two boundary points of the radial grid are the wall and the axis of the arc. The wall temperature T_w stays constant and is chosen as $T_1 = T_w$. The radius of this isothermal surface $r_1^2 = r_w^2$ does not change with time:

$$\partial r_1^2/\partial t = 0 . \quad (10)$$

The axial temperature T_A on the other hand is decreasing. The axis is not a point of constant temperature and must be treated separately.

As time increases isothermal radii are disappearing in the axis (see Figure 1). The isothermal surface disappearing in the axis at each time level is labelled $i = N$, i. e. the temperature T_N equals the axial temperature T_A at each time level. The number of radial grid points, N, is decreasing with time.

The difference between the temperature on the axis T_N, and the temperature T_{N-1} of the neighbouring isothermal surface does not equal the chosen constant value ΔT, but depends on time. Therefore the common formulae of an equal finite difference system cannot be applied in the region neighbouring the axis.

For the grid points $i=N$ and $i=N-1$ the variation of the different physical quantities with the radial coordinate, i. e. the temperature, are computed using a series expansion of T in r^2, where all but three terms are dropped.

The time variation of the isothermal radius r_N^2 is directly given by Eq. (8) since the radial mass velocity is zero on the axis:

$$v_M(r^2=0)=0,$$
$$\partial r_N^2/\partial t=(\partial r^2/\partial t)_{r^2=0}=-(q/\pi\varrho)_{r^2=0}. \quad (11)$$

From this the variation of the axial temperature T_A with time can be determined:

$$dT_A/dt=-(\partial T/\partial r^2)_{r^2=0}(\partial r^2/\partial t)_{r^2=0}. \quad (12)$$

Once the values of q_i are computed at each grid point of a certain time level, $(\partial r^2/\partial t)_{r^2=0}$ as well as $(\partial r_1^2/\partial t)$ are known quantities according to Eqs. (10) and (11). One of the two values is used as a starting point to compute the time variation of all isothermal radii, $\partial r_i^2/\partial t$, according to Equation (10). The second one is used to determine dp/dt. To do this one has to compute all values of q_i and $\partial r_i^2/\partial t$ in two parts.

$$q_i=a_i+b_i(dp/dt),$$
$$\partial r_i^2/\partial t=\alpha_i+\beta_i(dp/dt). \quad (13)$$

If all coefficients a_i, b_i, α_i and β_i are known, the equation $\partial r_1^2/\partial t=0$ for instance yields the value dp/dt.

In Eq. (8 a) there appear derivatives with respect to the radial coordinate. In the isothermal representation they are given by:

$$\frac{\partial F}{\partial r^2}=\frac{1}{\partial r^2/\partial T}\frac{\partial F}{\partial T}=\frac{1}{\partial r^2/\partial T}\frac{F_{i+1}-F_{i-1}}{2\Delta T},$$
$$\frac{\partial r^2}{\partial T}=\frac{r^2_{i+1}-r^2_{i-1}}{2\Delta T}. \quad (14)$$

For reasons of numerical stability the second derivative with respect to temperature must be isolated in the term describing the divergence of the heat flux vector:

$$\frac{\partial}{\partial r^2}\left(r^2\varkappa\frac{\partial T}{\partial r^2}\right)=\frac{1}{\partial r^2/\partial T}\left[\varkappa+\frac{r^2}{\partial r^2/\partial T}\frac{d\varkappa}{dT}-\frac{r^2\varkappa}{(\partial r^2/\partial T)^2}\frac{\partial^2 r^2}{\partial T^2}\right]. \quad (15)$$

In discrete form the second derivative reads:

$$\left(\frac{\partial^2 r^2}{\partial T^2}\right)_i=\frac{r^2_{i+1}-2r_i^2+r^2_{i-1}}{(\Delta T)^2}. \quad (16)$$

V. Numerical Stability

The special choice of grid points in the isothermal representation becomes advantageous only if the stability of the computation is not made much worse in the transition to the new coordinate system. In this chapter therefore we investigate the numerical stability of the isothermal system.

If the basic equations are put in discrete form using grid points which are equidistant in temperature, i. e. with $\Delta T=\text{const}$, the radial distance, Δr, between two neighbouring grid points can become extremely small in certain arc regions. This implies a severe limitation on the possible time step Δt if the common two level explicit schemes are used for the computation of the unknown quantities at the advanced time level t_{j+1}, starting from the already known distribution at the time level t_j:

$$r^2_{i,j+1}=r^2_{i,j}+\Delta t(\partial r_i^2/\partial t)_j. \quad (17)$$

This method is numerically unstable unless Δt is smaller than the value given by the von Neumann condition. In isothermal representation this condition reads:

$$\Delta t\leqq\Delta t_{max}=\frac{(\Delta T)^2}{2}\frac{\varrho c_p}{\varkappa}\left(\frac{\partial r}{\partial T}\right)^2. \quad (18)$$

If this limiting value is computed locally, i. e. over the arc cross section, extremely small values of Δt_{max} appear in the arc region close to the wall. These would require an injustifiably high computing time.

These instabilities can still be removed even using an explicit method, if the three level scheme due to DU FORT and FRANKEL [14] is applied, where the central term in Eq. (16), $2r^2_{i,j}$, is replaced by $r^2_{i,j-1}+r^2_{i,j+1}$. There are two disadvantages to this method in our case. For time steps about one order of magnitude larger than the value given by Eq. (18) the method also becomes instable. Furthermore, an extremely high precision in the computation is necessary.

In our computations we therefore used an implicit two level scheme of the type described for instance in [14]. This method is stable for any time step Δt, so that the value of Δt is limited only by the

desired accuracy of the results. In this method an equation is set up for each radial mesh point which contains, in linear form, three unknown values of the quantity required at the advanced time level. The corresponding matrix is inverted using a tri-diagonal solution method [15].

In the two level scheme used here the quantities required at the advanced time level are given by [14]:

$$r^2_{i,j+1} = r^2_{i,j} + \Delta t\left[(1-\theta)\left(\frac{\partial r_i^2}{\partial t}\right)_j + \theta\left(\frac{\partial r_i^2}{\partial t}\right)_{j+1}\right], \quad (19)$$

To ensure stability $0.5 \leqq \theta \leqq 1$. In our example $\theta = 0.5$ did yield stable behaviour.

It is assumed that at the time level t_j the radial distribution of all quantities, and therefore also the values $r^2_{i,j}$ and $(\partial r_i^2/\partial t)_j$, is known. The expressions $(\partial r_i^2/\partial t)_{j+1}$ on the other hand, at an advanced time level depend in a very complicated way on the unknown radii $r^2_{i,j+1}$. As the numerical instability is caused by the second derivative with respect to the radial coordinate, i. e. the term given in Eq. (16), it is sufficient to treat only the isothermal radii appearing in Eq. (16) as unknown quantities at the advanced time level. All other expressions in $(\partial r_i^2/\partial t)_{j+1}$ containing the isothermal radii $r^2_{i,j+1}$ are computed using values of $r^2_{i,j+1}$ which have been determined in an explicit way (for instance by putting $\theta = 0$). In this case four unknown radii $r^2_{i,j+1}$ appear in linear form in each of the Eq. (18). But if the area between two neighbouring isothermal surfaces

$$A_i = \pi(r^2_{i-1} - r^2_i) \quad (20)$$

is introduced instead of the radii r_i^2, only three unknown values, $A_{i,j+1}$, appear in each equation. The matrix representing the system of Eq. (19) is then tri-diagonal and can be inverted according to known methods [15]:

$$-\alpha_i A_{i+1} + \beta_i A_i - \gamma_i A_{i-1} = \delta_i. \quad (21)$$

Here the areas A_i are the quantities required at the advanced time level t_{j+1}. All matrix elements α_i, β_i, γ_i, δ_i are known as they are computed using radii $r^2_{i,j+1}$ determined in an explicit way.

In the isothermal representation the boundary values must be included in a special way. The inversion of the matrix (21) is therefore described in detail.

The matrix is inverted introducing [15]

$$A_i = w_i A_{i+1} + g_i \quad (22)$$

where the coefficients

$$w_i = \frac{\alpha_i}{\beta_i - \gamma_i w_{i-1}}, \qquad g_i = \frac{\delta_i + \gamma_i g_{i-1}}{\beta_i - \gamma_i w_{i-1}}$$

can be computed as w_2, and g_2 can be determined directly from the area next to the wall

$$w_2 = \alpha_2/\beta_2, \qquad g_2 = \delta_2/\beta_2.$$

One further boundary condition must be used to determine the highest i-value of the A_i. In our case this is the condition

$$\sum A_i = \pi r_1^2.$$

In the isothermal representation the temperature difference between the axis and the neighbouring isothermal surface r^2_{N-1} does not equal the constant step ΔT. Therefore at the grid point $i = N-1$, Eq. (16) cannot be applied and Eq. (19) cannot be written in the form (21). For this reason the value $r^2_{N-1,j+1}$ is computed according to Eq. (19) where all radii appearing in $(\partial r^2_{N-1}/\partial t)_{j+1}$ are determined in an explicit way. The second boundary condition is then:

$$\sum_{i=2}^{N-1} A_i = \pi(r_1^2 - r^2_{N-1}).$$

If the abbreviations

$$S_i = 1 + w_{i-1} S_{i-1},$$
$$G_i = G_{i-1} + g_i S_i$$

are used with

$$S_2 = 1, \qquad G_2 = g_2$$

there follows

$$\sum_{i=2}^{N-1} A_i = \pi(r_1^2 - r^2_{N-1}) = G_{N-2} + S_{N-1} A_{N-1}.$$

From this equation A_{N-1} can be determined and subsequently, with Eq. (22), all other areas A_i.

The described method yields numerical stability in our computation as long as the computed quantities do not change too much within one time step. In the case of very strong variations within one time step one single iteration of the whole procedure ensures numerical stability. In this case the coefficients of the matrix (21) are computed using, in the second step, the radii determined in the first step of the iteration procedure.

VI. Computation of a Decaying Nitrogen Arc

As a specific example of the method described above the decay, after current interruption, has been

computed for a 5 mm ϕ, wall-stabilized arc which carries a current of 100 A in 1 atm nitrogen. The stationary arc corresponding to the chosen values is described in detail in [4]. The temperature variations of all material functions are known from theory as well as from experiment [16, 4]. The pressure dependence of the mass density and the electrical conductivity have been taken into account exactly. The pressure dependence of the thermal conductivity and the specific heat on the other hand has nearly no influence on the decay of the arc in the range considered here and has been included only in an approximate way.

In the first period after arc interruption the energy transport by radiation plays an important role. In the core of the arc it even exceeds the conductive transport. For the stationary arc the radial distribution of the balance of radiative power per unit volume, u, is known [4, 17]. It can be split into an emission, e, of radiative power which is contributing to the radiative transport and into a corresponding absorption, a, of radiative power [see Eq. (3)]. With falling temperature the emission of radiation strongly decreases and so does the absorption. The emission, $e(T)$, decreases according to the known temperature dependence. Due to the special temperature dependence of the coefficient of absorption the emitted energy is at all stages of the decay absorbed mainly in arc regions corresponding to the same temperature. But as the total amount of emitted energy decreases, less energy can be absorbed with increasing time.

To take into account the change with time of the radiative transport without exactly solving the radiation transport equation for every time step, a special assumption is made: The temperature variation of the absorption, $a(T)$, stays the same as in the stationary arc, but the absolute values of $a(T)$ decreases in such a way that at all stages of the decay the same proportion of the emitted energy is reabsorbed within the arc. In the chosen arc about 85% of the emitted energy is reabsorbed. The introduction of a pressure dependence of the radiative term did not change the results noticeably.

The decay of the temperature profile within the first 100 μsec after arc interruption has been computed using temperature steps $\Delta T = 250\ ^\circ\mathrm{K}$ and a wall temperature $T_w = 500\ ^\circ\mathrm{K}$. This corresponds to 55 radial grid points in the initial distribution. The time step chosen was $\Delta t = 2.5 \times 10^{-7}$ sec for the range $0 \leqq t \leqq 35$ μsec and $\Delta t = 5 \times 10^{-7}$ sec for the range $35 \leqq t \leqq 100$ μsec. The CPU-time necessary to compute these 270 time steps on an IBM 370/155 was 37 sec.

The movement of some of the isothermal radii towards the arc center is shown in Figure 1. The radial temperature distribution as well as the time-variation of temperature can be deduced from this picture at any time level.

To analyse the origin of this movent, i. e. of the temperature decrease, the physical effects contributing to $-\partial r^2/\partial t$ are separated in Figs. 2 a – c for different time levels after current interruption. The displacement of the isothermal surfaces can be split into the velocity of the isothermal surfaces relative to mass, v_{IM}, and into the mass velocity itself, v_M [see Eq. (8)].

The flow of mass relative to the isothermal surfaces, q, is caused by three physical effects, radiation, thermal conduction and work of compression, as can be seen from Equation (8 a). The contribu-

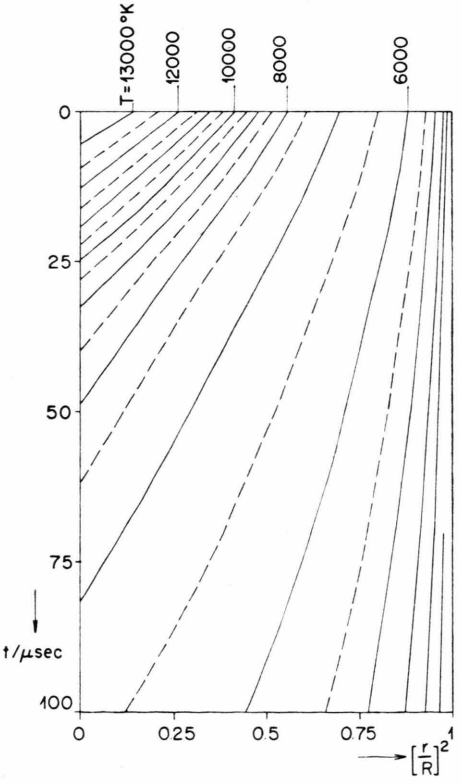

Fig. 1. Position of squared isothermal radii $r^2(T_i, t)$ as a function of time. Solid lines indicate radii corresponding to $T_k = k \cdot 1{,}000\ ^\circ\mathrm{K}$, broken lines indicate radii corresponding to $T_{k'} = T_k + 500\ ^\circ\mathrm{K}$.

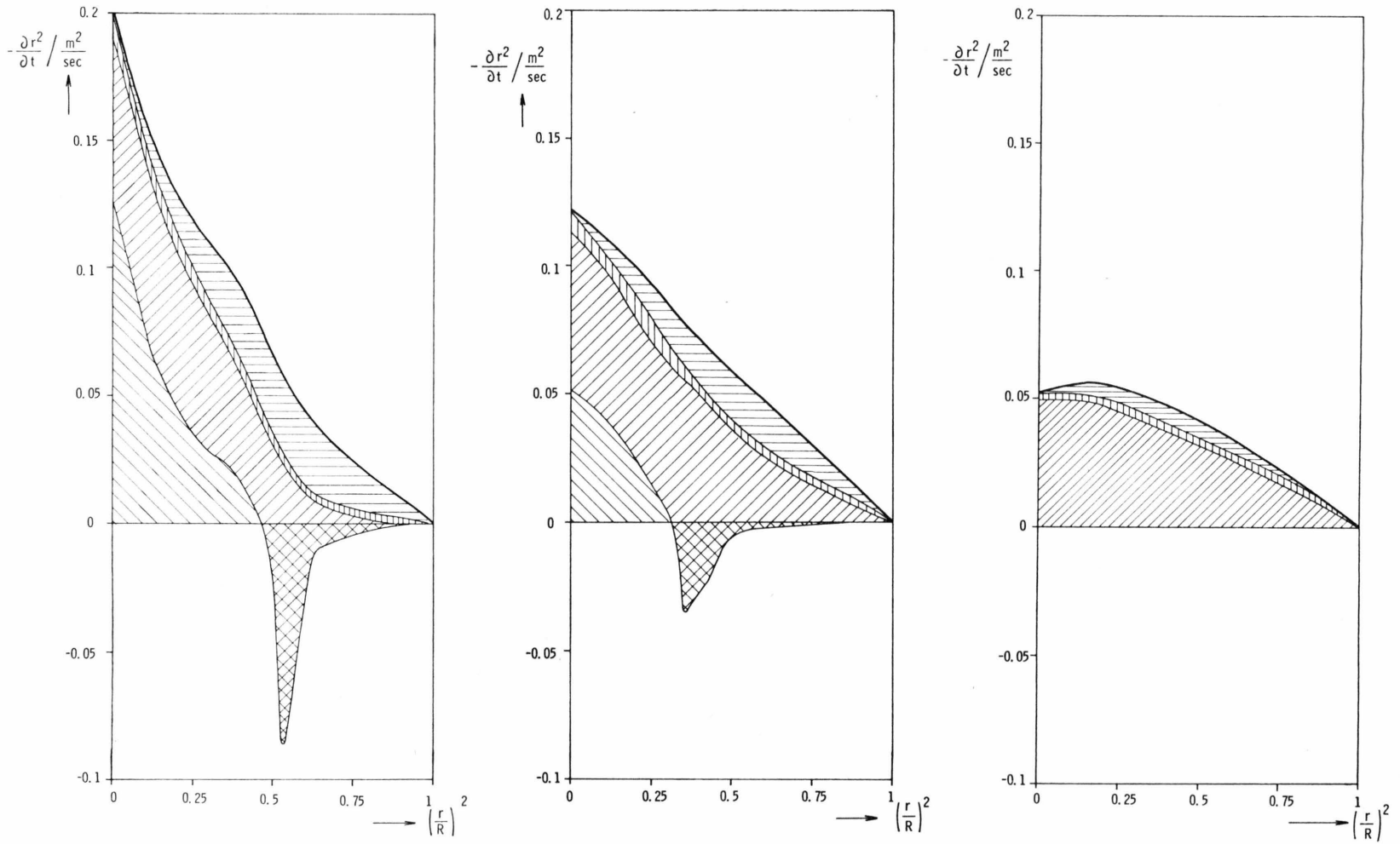

Fig. 2. Local time variation of square isothermal radii, split into the four contributing physical processes.
Contribution of radiation:
conduction:
work of compression:
mass flow:
a) Immediately after current interruption, b) after the time $t=15$ μsec, c) after the time $t=70$ μsec.

tion of all four terms is indicated by hatching in Figures 2 a – c. Immediately after arc interruption (Fig. 2 a) the emission of radiation dominates in the core of the arc inducing a strong movement of isothermal radii towards the axis. The absorption of radiative energy becomes especially effective in arc regions with temperatures below 10 000 °K. There gas is heated up by radiation and the radiative term alone would induce a displacement of isothermal lines towards the wall (negative contribution to $-\partial r^2/\partial t$). Thermal conduction plays an important role all over the cross section. In the low temperature region it compensates the heating due to radiative absorption. The share of the pressure-volume work is nearly negligible. The contribution of the pure mass flow is especially high near the wall. There the temperature distribution is carried with the mass flow ($v_{MI} \ll v_M$), while in the core of the arc the displacement is mainly due to the movement of isothermal surfaces relative to the mass ($v_{MI} \gg v_M$).

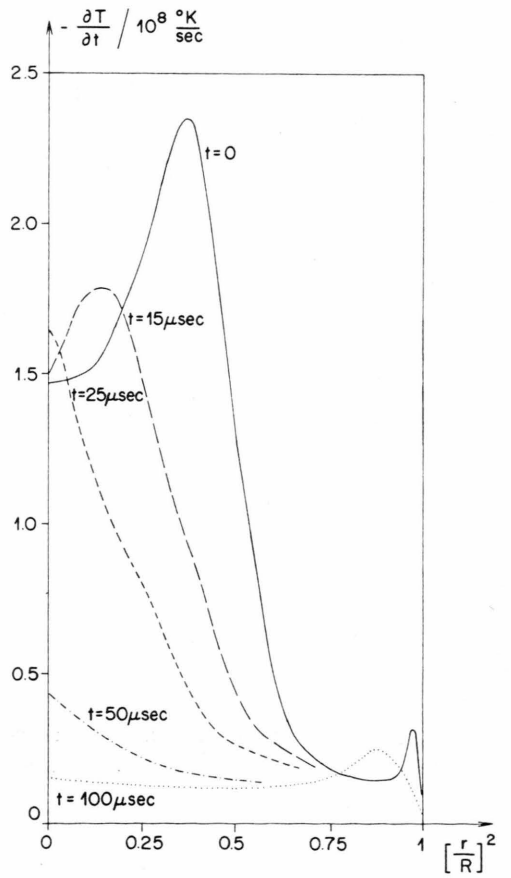

Fig. 3. Local variation of temperature with respect to time at different time levels after current interruption.

With passing time (Fig. 2 b, c), i. e. with falling temperature, the radiative transport strongly decreases. The displacement of isothermal radii is then mainly due to thermal conduction. The volume-pressure contribution remains almost constant and the effect of the pure mass flow becomes less important.

The local variation of temperature with time is plotted against the squared radius in Figure 3. It is given by the product of the velocity of isothermal radii times the radial temperature gradient:

$$\frac{\partial T}{\partial t} = -\frac{\partial T}{\partial r^2}\frac{\partial r^2}{\partial t}. \tag{23}$$

While the quantity $-\partial r^2/\partial t$ increases continuously towards the axis, the gradient $\partial T/\partial r^2$ has especially high values close to the wall and in the arc region, with temperatures around 10 000 °K, corresponding to the low values of the thermal conductivity in the valley between the ionisation and dissociation peak. In these two regions there are maxima in the $-\partial T/\partial t$-curve, i. e. there the temperature varies especially strongly with time.

Radial temperature distributions, as derived from Fig. 1 for different time levels, are drawn in Figure 4.

In Fig. 5 the variations of the axial temperature and the pressure with time are shown. Approximately 30 μsec after current interruption the rate of decrease of both pressure and axial temperature reduces, but it is more pronounced in the case of the latter. This is the time at which the contributions of radiative transport nearly disappear and the low value of the thermal conductivity around $T = 10\,000$ °K becomes effective in the core.

A quantity which is of special importance in the description of the behaviour of electric arcs is the electrical conductance G:

$$G = I/E = \pi \int_0^{R^2} \sigma \, dr^2. \tag{24}$$

With falling temperature the electrical conductance decreases too:

$$\frac{dG}{dt} = \pi \int_0^{R^2} \frac{\partial \sigma}{\partial t} dr^2; \quad \frac{\partial \sigma}{\partial t} = \frac{d\sigma}{dT}\frac{\partial T}{\partial t}. \tag{25}$$

To show which arc regions contribute most to the decay of the conductance at different time levels,

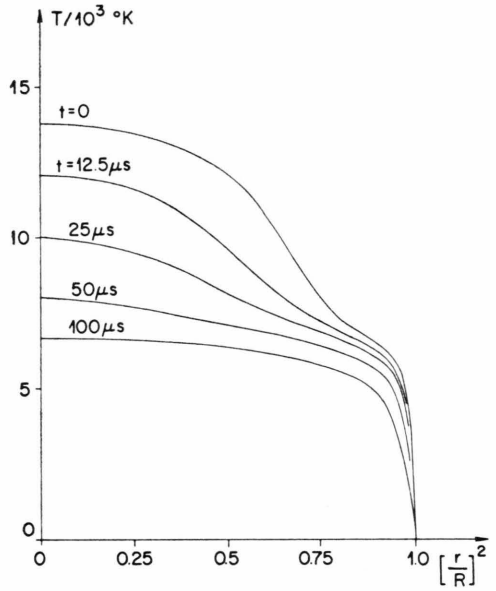

Fig. 4. Radial temperature profiles at different time levels.

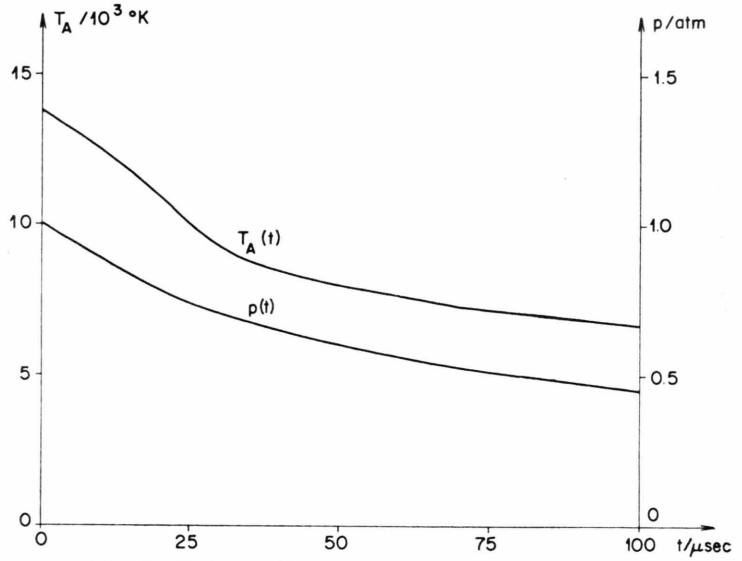

Fig. 5. Variation of pressure and axial temperature with respect to time.

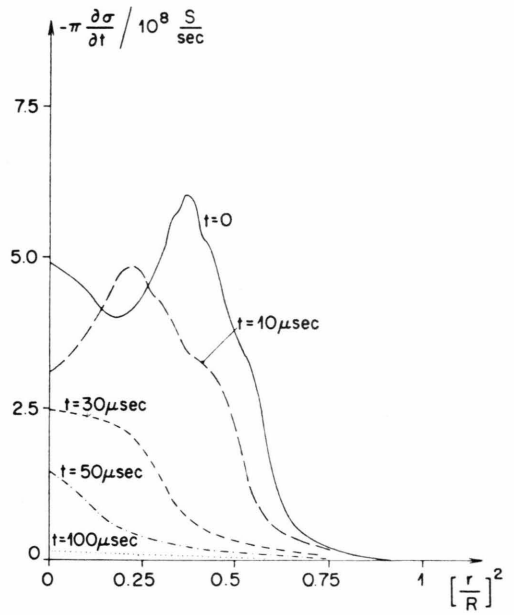

Fig. 6. Local variation of electrical conductivity with respect to time at different time levels after current interruption.

$-\pi\,\partial\sigma/\partial t$ is plotted against r^2 in Figure 6. After a time of about 30 μsec, when the peak in $-\pi\,\partial\sigma/\partial t$ corresponding to a temperature of approximately 10 500 °K has disappeared in the axis the decrease of the electrical conductance is slowed down. The four physical effects separated in Fig. 2 contribute to $-\pi\,\partial\sigma/\partial t$ and $-\partial T/\partial t$ in the same proportion as they do to $-\partial r^2/\partial t$.

For the special arc described in this chapter the decay of the electrical conductance after arc interruption had been measured by HERTZ [10]. His experimental curve is drawn in Fig. 7 as a dotted line and the result of our computation as a solid line. For this computation we used an experimental curve for the electrical conductivity $\sigma(T)$ as derived from measurements on a wall stabilized arc at a pressure of 1 atm [4, 18]. For the pressure variation of the electrical conductivity we used the dependence which is given by the curves of YOS [16].

For comparison the decay of the conductance, $G(t)$, has been computed using the theoretical values of $\sigma(T)$ as given by FRIE and HERTZ [10, 19] at a pressure of 1 atm and again applying the pressure variation due to YOS [16]. The result is drawn in Fig. 7 as a broken line. Over almost the whole time range covered in our computation the experimental curve runs between the two theoretical curves. This shows that the deviation of the theoretical result from the experimental curve is not greater than the uncertainty in the basic material functions.

In the range $t > 70$ μsec the $G(t)/G_0$ curve using theoretical $\sigma(T)$-values runs far below the one using experimental $\sigma(T)$-values. This is due to the fact that in the temperature range below 8000 °K the

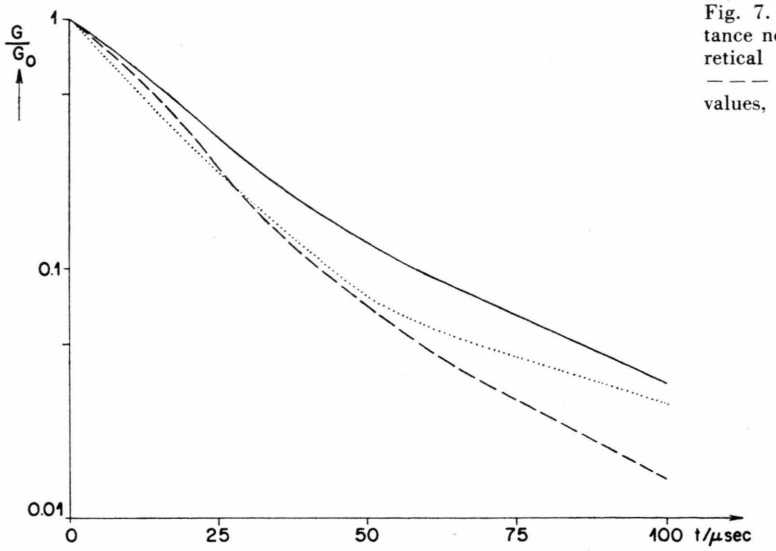

Fig. 7. Time variation of the electrical conductance normalized to its initial value. ——— theoretical result using experimental $\sigma(T)$-values, — — — theoretical result using theoretical $\sigma(T)$-values, ····· experimental result of HERTZ [10].

theoretical $\sigma(T)$ values, as given by Frie and Hertz or by Yos, are much smaller than the experimental $\sigma(T)$-values. The decay of the conductance in the range $t > 70$ μsec, as measured by Hertz, indicates that below 8000 °K the electrical conductivity $\sigma(T)$ might decrease with falling temperature even less than the experimental $\sigma(T)$-curve we used, i. e. much less than the $\sigma(T)$-curve given by theory.

Close correspondence between experimental and theoretical results has been achieved without the drastic assumption of severe Non-LTE-processes in the low temperature region, as postulated by HERTZ [10].

Acknowledgements

Thanks are due to Dr. K. RAGALLER for several discussions on the subject and to Miss D. SELIG for her assistance in the computer calculations.

[1] H. MAECKER, Z. Phys. **158**, 392 [1960].
[2] J. UHLENBUSCH, Z. Phys. **179**, 347 [1964].
[3] U. PLANTIKOW and S. STEINBERGER, Z. Phys. **231**, 109 [1970].
[4] W. HERMANN and E. SCHADE, Z. Phys. **233**, 333 [1970].
[5] J. C. MORRIS, R. P. RUDIS, and J. M. YOS, Phys. Fluids **13**, 608 [1970].
[6] R. WIENECKE, Z. Phys. **146**, 39 [1956].
[7] R. HOLMES and G. R. JONES, Z. Phys. **215**, 466 [1968].
[8] R. L. PHILLIPS, Z. Phys. **211**, 113 [1968].
[9] L. DETLOFF, Dissertation Techn. Hochschule Aachen 1969.
[10] W. HERTZ, Z. Phys. **245**, 105 [1971].
[11] H. MAECKER, Proc. IEEE **59**, 4 [1971].
[12] K. RAGALLER, W. R. SCHNEIDER, and W. HERMANN, ZAMP **22**, 920 [1971].
[13] W. HERMANN, U. KOGELSCHATZ, K. RAGALLER, and E. SCHADE, Phys. Fluids, to be published [1973].
[14] R. D. RICHTMYER and K. W. MORTEN, Difference Methods for Initial-Value Problems, Interscience Publishers, New York 1967.
[15] A. R. MITCHELL, Computational Methods in Partial Differential Equations, John Wiley & Sons, London 1969.
[16] J. M. YOS, Technical Documentary Report No. ASD T DR-62-729, revised version 1967.
[17] W. HERMANN and E. SCHADE, J. Quant. Spectr. Rad. Transfer **12**, 1257 [1972].
[18] U. PLANTIKOW, Z. Phys. **237**, 388 [1970].
[19] W. FRIE, Z. Phys. **201**, 269 [1967].